



# Parabolized stability analysis of dual-stream jets

Aniruddha Sinha<sup>1\*</sup>, Datta V. Gaitonde<sup>2†</sup> and Nikhil Sohoni<sup>1‡</sup>

<sup>1</sup>*Aerospace Engineering, Indian Institute of Technology Bombay, Powai, Mumbai 400076, INDIA*

<sup>2</sup>*Mechanical and Aerospace Engineering, The Ohio State University, Columbus, OH 43210, USA*

We model coherent wavepackets in turbulent, axisymmetric, dual-stream jets as linear instabilities of the time-averaged flow field thereof. For this, we use linear parabolized stability equations (PSE) that account for the slowly varying nature of the base flow in the axial direction. The procedure is evaluated with base flows derived from large-eddy simulation (LES) of subsonic dual-stream jets operated at two conditions – Case 2 has steeper gradients in the inner shear layer due to a faster core stream compared to Case 1, and both have heated core streams but isothermal secondary streams. Owing to the presence of two shear layers (especially distinct near the nozzle), both jets support two unstable modes that are called inner and outer modes. Separate PSE calculations are initiated for the two different modes. The outer mode is found to stabilize earlier, subsequent to which, the PSE must be terminated to prevent the solution from merging with the inner mode that remains unstable farther downstream. The inner mode PSE solution can be run till the downstream end of the data domain. The PSE solution's pressure component, which displays the wavepacket nature most clearly, is validated against the LES data after the latter is filtered for its coherent part using proper orthogonal decomposition. In Case 2, both inner and outer modes are observed to agree reasonably well with separate coherent modes of the data. Case 1, with its weaker inner shear layer, has only the outer modes comparing well with the filtered data.

## I. Introduction

Dual-stream jets are most commonly seen in turbofan jet engines on civilian aircraft. The core stream is generally hotter and at higher speed with the cooler low-speed stream forming an annular jet around it. High bypass ratios (BPR) (ratio of annular stream mass flux to that of core stream) in turbojet engines have not only made them much more efficient, but have also yielded significant reduction of turbulent mixing noise. One of the approaches proposed to reduce the noise further is to offset the two nozzles; this would preferentially decrease the noise radiated to critical sectors (typically towards the ground and/or aircraft cabin).<sup>1</sup> Techniques are needed to rapidly predict the noise radiated from various such designs. In this paper, we pursue the reduced-order modeling of noise sources in coaxial dual-stream jets as a step towards this ultimate goal.

The aft sector of jet engines is typically the loudest under usual operating conditions, the spectrum thereof being dominated by low frequencies and low azimuthal Fourier modes.<sup>2</sup> This component of turbulent mixing noise has been linked to the dynamics of coherent large-scale structures (coherent wavepackets in Fourier domain) observed in the jet plume.<sup>3</sup> The overall stochastic features of these structures, like the average amplitude envelope in the stream direction and their average phase speed, are well replicated by *linear* instability waves of the turbulent mean flow of the jet.<sup>3</sup> Although this central idea is several decades old,<sup>4,5,6</sup> it was not until the recent marked advances in experimental and computational capabilities that it obtained direct empirical validation in high-speed high-Reynolds number *single-stream* axisymmetric jets.<sup>7,8,9,10</sup>

The first study that applied the idea of modeling coherent wavepackets as instabilities of the turbulent mean flow to *dual-stream* jets was reported in Ref. 11, wherein the method of multiple scales<sup>12</sup> was used. Wavepackets with supersonic phase speeds are very efficient radiators of noise, and the above technique in

\*Assistant Professor; AIAA Member; Corresponding author: as@aero.iitb.ac.in

†John Glenn Professor; AIAA Fellow

‡Graduate student

conjunction with acoustic continuation methods was used effectively to predict the noise in a supersonic coaxial jet.<sup>13</sup> Classical parallel-flow spatial linear stability theory (LST) was also applied to a family of mean flow profiles to understand the influence of various mean flow parameters on the noise radiation.<sup>14,15</sup> Of late, the parabolized stability equations (PSE) that account for mild non-parallelism of the base flow, has been used in coaxial jets.<sup>16</sup>

An extensive program of research was undertaken in the framework of the European project CoJeN (Computation of Coaxial Jet Noise) to understand the fluid dynamics and acoustics of dual-stream jets of realistic geometries, bypass ratios and temperatures. Under CoJeN, an experimental program was undertaken to characterize the near hydrodynamic field of coaxial jets.<sup>17</sup> A practically relevant configuration consisting of a center-body within the core jet (the so-called ‘short cowl nozzle’) was tested. One of the outcomes was the observation of large coherent domains in the pressure field of the complex jets, similar to those observed in single-stream jets. This motivates the extension of the instability wave-based models to dual-stream jets. Several well-resolved large-eddy simulations (LES) have also been performed recently.<sup>18,19,20</sup> These empirical databases have provided significant support to the modeling efforts.

In this paper, we report on a detailed validation of a PSE model using a new LES database of the short-cowl dual-stream nozzle configuration at two operating conditions. In some respect, the present work resembles that reported in Ref. 16. However, we pursue a more extensive validation study to understand the appropriateness (and limitations) of the modeling approach. Once the model is validated, it may be used for exploring the parameter space of nozzle geometry and operating conditions – a very high-dimensional space.

## II. Linear parabolized stability equations for axisymmetric jets

Classical parallel flow spatial linear stability theory (LST) assumes that the base flow does not change in the stream direction – a constraint that is an acceptable approximation for high-speed high-Reynolds number shear layers. On the other hand, parabolized stability equations (PSE) account for slow variations in the base flow in the stream direction, in a computationally efficient manner.<sup>21</sup> If neither of these assumptions are valid in a particular setting then one has to resort to global stability analysis, which is computationally expensive.

In LST, the ansatz for the stability solution consists of a wave in the stream direction, say  $x$  direction, that has uniform growth or decay (constant complex wavenumber). In PSE, however, both the wave shape (in the cross-stream plane) as well as the wavenumber are allowed to have mild variations in the  $x$  direction, commensurate with the variations in the base flow.

PSE (as well as LST) was originally intended to study transition in *laminar* flows dominated by shear. Of late, PSE is being used to model coherent wavepackets (large-scale structures in the Fourier domain) in free shear flows (e.g., jets) as linear perturbations of the *turbulent* mean flow field.<sup>8,3</sup> This model hypothesizes a separation of scales between the coherent fluctuations and the remaining incoherent (fine-scale) turbulence, the latter being assumed to be indirectly effective in establishing the mean flow. Although such a hypothesis has not been proven conclusively in high-speed jets, there are empirical indications that the low-frequency low-azimuthal-mode fluctuations of interest in acoustics have significantly lower energy compared to the overall turbulent kinetic energy, and hence may be indeed in the linear regime.<sup>9</sup> In fact, PSE models have delivered encouraging agreement with empirically-observed coherent wavepackets in high-speed high-Reynolds number jets.<sup>8,9,10,22</sup>

For details of the linear PSE theory, the reader is referred to Refs. 8,10; here we give a very brief description. The flow field of the jet is described in cylindrical coordinates  $\mathbf{x} = (x, r, \theta)$  by  $\mathbf{q} = (u_x, u_r, u_\theta, p, \zeta)^T$ , which respectively denote the axial, radial and azimuthal components of velocity, pressure, and specific volume. Stability analysis decomposes  $\mathbf{q}$  into a steady base flow  $\bar{\mathbf{q}}$  (herein it is the turbulent mean flow), and the residual fluctuations  $\mathbf{q}'$ . Given the time-stationarity and azimuthal periodicity and homogeneity of the fluctuations, linear PSE represents them with the ansatz

$$\mathbf{q}'(\mathbf{x}, t) = \hat{\mathbf{q}}_{\omega, m}(x, r) e^{i(m\theta - \omega t)} + \text{c.c.}, \quad \hat{\mathbf{q}}_{\omega, m}(x, r) = \underbrace{e^{i \int_{x_0}^x \alpha_\omega(\xi) d\xi}}_{=:\chi_\omega(x)} \tilde{\mathbf{q}}_{\omega, m}(x, r). \quad (1)$$

In the above,  $\hat{\mathbf{q}}$  is the temporal and azimuthal Fourier coefficient of  $\mathbf{q}'$ , with circular frequency  $\omega$  and azimuthal mode number  $m$ . It is decomposed into the slowly-varying (in  $x$ ) shape function  $\tilde{\mathbf{q}}$  and the rapidly-varying wave-like part  $\chi$  (with wavenumber  $\alpha$  having slow variations in  $x$  again). For later reference,

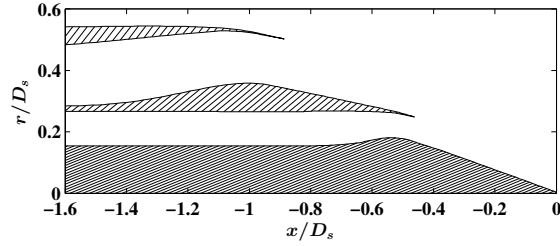


Figure 1. The geometry of the axisymmetric short cowl nozzle (SCN). Here,  $D_s$  is the diameter of the secondary nozzle at its exit.

Case	$U_p$ ( $a_p$ ) [m/s]	$U_s$ ( $a_s$ ) [m/s]	$T_p$ [K]	$T_s$ [K]	$U_s/U_p$	$Re_s$	$\delta ta_\infty/D_s$	$\Delta ta_\infty/D_s$	$\tau a_\infty/D_s$
Case 1	340 (556)	307 (340)	770	288	0.90	$5.6 \times 10^6$	$10^{-3}$	0.250	392.5
Case 2	397 (556)	250 (340)	770	288	0.63	$4.6 \times 10^6$	$5 \times 10^{-4}$	0.125	400

Table 1. Jet operating conditions, with  $U$ ,  $a$  and  $T$  denoting flow speed, sound speed and temperature respectively. The subscripts ‘ $p$ ’ and ‘ $s$ ’ refer to the primary and secondary streams’ exit conditions respectively. The Reynolds number  $Re_s$  is referred to the exit conditions of the secondary nozzle. The ambient temperature and pressure were  $T_\infty = 288$  K and  $p_\infty = 1$  bar in both cases. The simulation time step, sampling period and total duration are respectively  $\delta t$ ,  $\Delta t$  and  $\tau$ .

the real and imaginary parts of  $\alpha$ , denoted by  $\alpha_r$  and  $\alpha_i$ , are respectively associated with the wavelength and growth rate of the instability.

The above ansatz, when substituted in the governing equations (compressible Navier Stokes equations in cylindrical coordinates) linearized about the base flow, yields a partial differential equation (in  $x$  and  $r$ ). However, the assumption of slow variation in  $x$  renders the equation approximately parabolic in the convectively-unstable flows under consideration,<sup>21</sup> so that it can be marched in  $x$  starting from an initial condition at  $x_0$  (generally near the nozzle) using step sizes that are restricted in their lower bound.<sup>23</sup> The initial condition is invariably the unstable Kelvin-Helmholtz (K-H) mode found in the parallel-flow LST applied to the mean flow profile at  $x_0$ .

In a single-stream jet, there is a single K-H mode for a given  $x - \omega - m$  triplet owing to the single inflection point in the base flow profile. However, the dual-stream jet mean flow profile is more complex near the nozzle, and typically two K-H modes are found. These are referred to as inner and outer modes, since they peak at the inner and outer shear layers, respectively.<sup>15</sup> The PSE calculation can be initiated from either unstable mode to trace the respective mode’s streamwise evolution.<sup>16</sup>

### III. Large-eddy simulation database of dual-stream jet

The LES method employs a validated third-order upwind-biased scheme with a harmonic limiter in the streamwise and radial direction,<sup>24</sup> and a sixth-order compact difference method and eighth-order filter in the azimuthal direction.<sup>25</sup> Viscous terms are also evaluated with the sixth-order method. The geometry of the nozzle is the short cowl variety adopted from Ref. 17 (see fig. 1). It has a contoured center-body within the primary stream, and is representative of realistic jet engine exhausts. Note that all length dimensions are normalized by the diameter of the secondary nozzle exit, and the origin of the  $x$ -coordinate is at the tip of the center body. The primary and secondary nozzle diameters are respectively  $D_p = 0.134$  m and  $D_s = 0.273$  m.

Two operating conditions are simulated for the above nozzle using LES – these are detailed in table 1. Case 1 is the ‘condition 1’ of Ref. 17 whereas Case 2 is somewhat similar to ‘condition 2’ of Ref. 17 (the primary jet is similar but the secondary stream is slower). A comparative study of the behaviour of coherent wavepackets in the two cases will evince the effect of the velocity ratio.

A curvilinear structured grid is fitted to the nozzle geometry. It has 1075 and 593 points in the axial and radial directions respectively, with clustering on the two lip lines and near the nozzle exit. The azimuthal

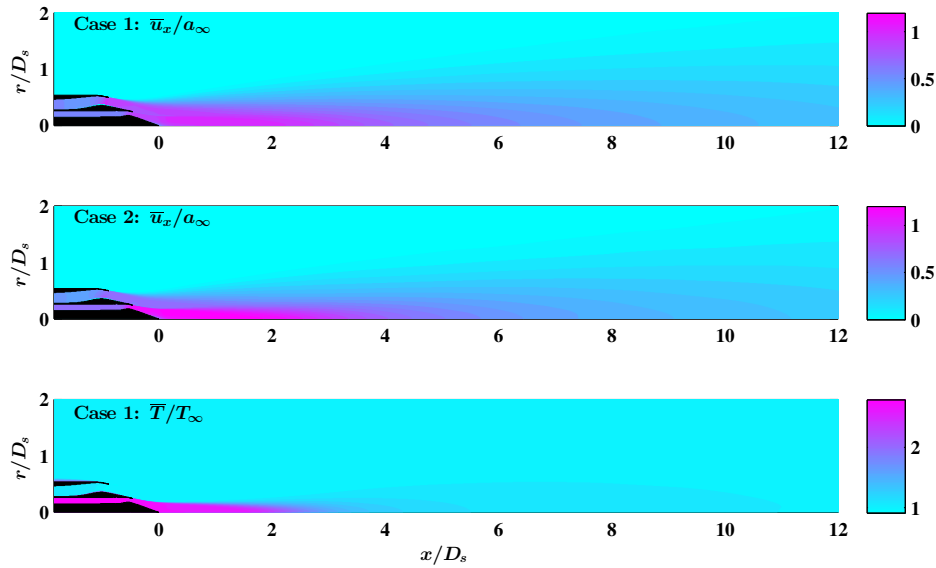


Figure 2. Time-averaged fields from LES. The average temperature field of Case 2 resembles that of Case 1.

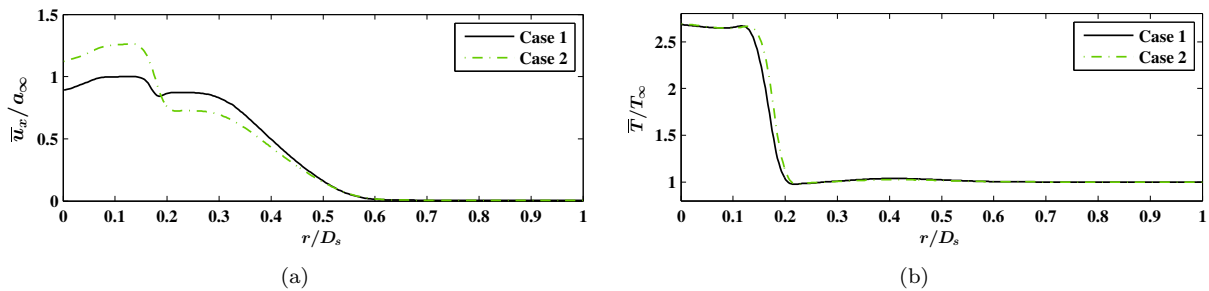


Figure 3. The average (a) axial velocity and (b) temperature ratio at  $x = 0.25D_s$  in the two cases.

grid is uniform with 100 points. The total comes to 64 million grid points. The grid is stretched beyond  $x > 8.15D_s$  and  $r > 3D_s$  to create appropriate sponge regions.

For reference, fig. 2 presents the time-averaged mean streamwise velocity and temperature fields in the two cases. Evidently, Case 2 displays the two velocity shear layers more distinctly. Both cases have a strong temperature shear layer between the primary and secondary streams.

## IV. Results

Since the PSE calculations are initiated from the unstable eigensolutions of LST applied at the initial station (chosen at  $x = 0.25D_s$ ), we first describe these instabilities in § A. The actual PSE solutions are presented in § B. All length dimensions are non-dimensionalized by  $D_s$ , and velocities by the ambient speed of sound  $a_\infty$ . However, we report the frequencies  $f$  in terms of the Strouhal number (referred to the secondary stream exit conditions) as  $St_s := fD_s/U_s$ .

### A. LST results at $x = 0.25D_s$

The LST is performed on the base flow extracted at  $x = 0.25D_s$ . The mean streamwise velocity and temperature profiles in the two cases at this axial station are shown in fig. 3. The presence of the center body results in a velocity deficit at the centerline. Apart from this, the axial velocity profiles are quite complicated with several inflection points, the two main ones being associated with the two shear layers

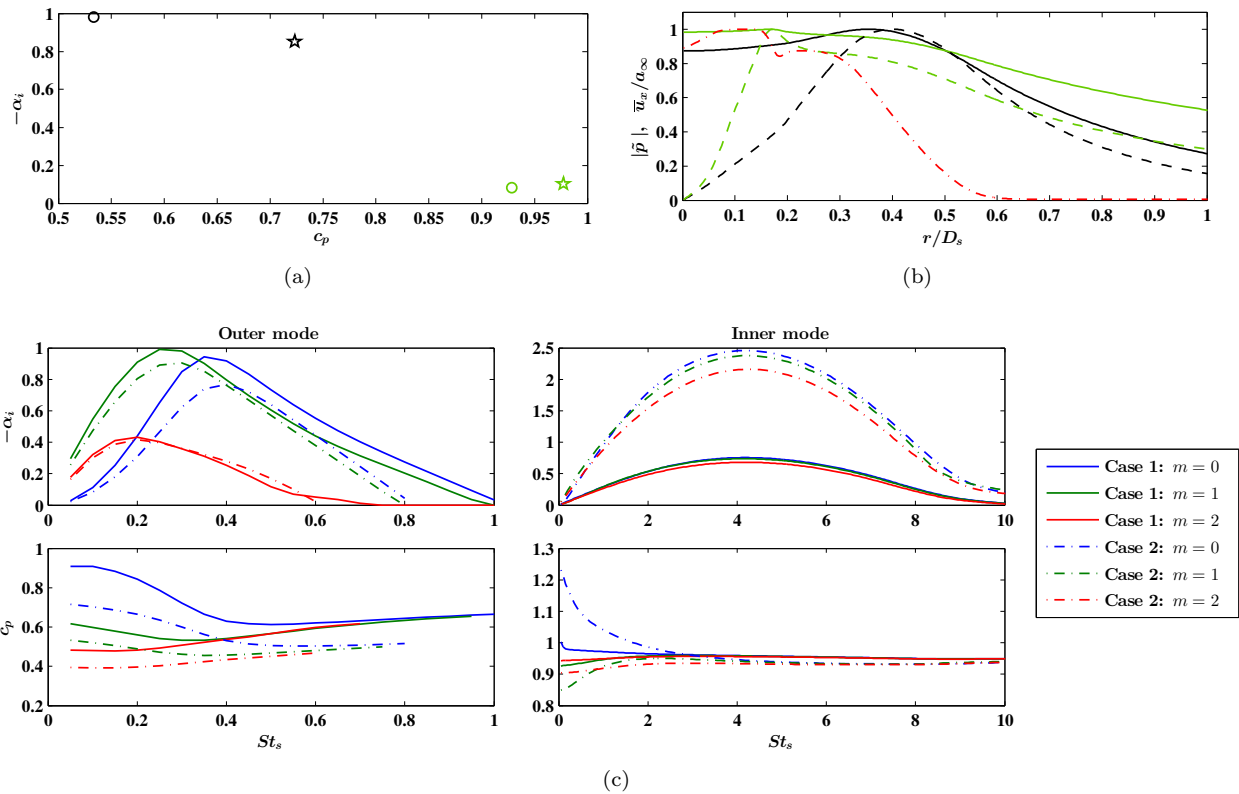


**Figure 4. (a)** Unstable LST eigenspectra from Case 1 in terms of the growth rate vs. phase speed at  $x = 0.25D_s$  for  $St_s = 0.3$  and  $m = 0$  and  $1$ . **(b)** Absolute values of LST pressure eigenfunctions for same modes. Stars or solid lines:  $m = 0$  mode; circles or dashed lines:  $m = 1$ ; green markers/lines: ‘inner modes’; black markers/lines: ‘outer modes’; red dash-dot line: local mean axial velocity profile. All curves are normalized by their respective maximum values over the radial domain. **(c)** Growth rates and phase speeds of the outer and inner LST eigenvalues for the pertinent range of Strouhal numbers and lowest two azimuthal modes.

(having maximum gradients). The velocity profile of Case 2 displays a sharper gradient in the inner shear layer, and a lower mean velocity at the outer inflection point – both observations are significant for the ensuing LST results. The temperature profiles of the two cases are very similar.

The unstable eigenvalues in Case 1 are presented in fig. 4(a) for a representative Strouhal number ( $St_s = 0.3$ ) in the axisymmetric ( $m = 0$ ) and the first helical ( $m = 1$ ) azimuthal modes. We note that at this axial station, one instability has low growth rate ( $-\alpha_i$ ) but high phase speed ( $c_p := \omega/\alpha_r/a_\infty$ ), whereas the other has higher growth rate with lower phase speed. The corresponding pressure eigenfunctions are presented in fig. 4(b). Following Ref. 15, we identify the first mode as the ‘inner mode’ (it peaks near the inflection point of the inner velocity shear layer where the temperature shear is also concentrated). The other is the ‘outer mode’ for corresponding reasons (there is no temperature shear near its peak). The higher axial velocity at the inner inflection point accounts for its higher phase speed.

The LST eigenvalues for both cases 1 and 2 are compiled in fig. 4(c) over the unstable range of Strouhal numbers and the three lowest azimuthal modes. The outer modes’ growth rates are substantially similar for the two cases. However, there is a slight reduction in instability in case 2 associated with the reduced shear between the secondary stream and the ambient therein (see fig. 3(a)). The phase speeds of the outer modes in Case 2 clearly reflect its reduced speed at the outer inflection point. The inner mode displays instability up to much higher values of  $St_s$  in both cases. There are two reasons for this. For one, the appropriate non-dimensional frequency for this instability is  $St_p := fD_p/U_p$ , which would dilate the abscissa. Moreover, fig. 3(a) shows that the shear in the inner layer is stronger than that in the outer layer. Among the two cases, Case 2 displays a much higher shear between the two streams, and this is reflected in the significantly enhanced growth rate of its inner mode compared to Case 1. The phase speeds of the inner mode are comparable, except at low frequencies. The  $m = 2$  outer mode is consistently more stable than the other

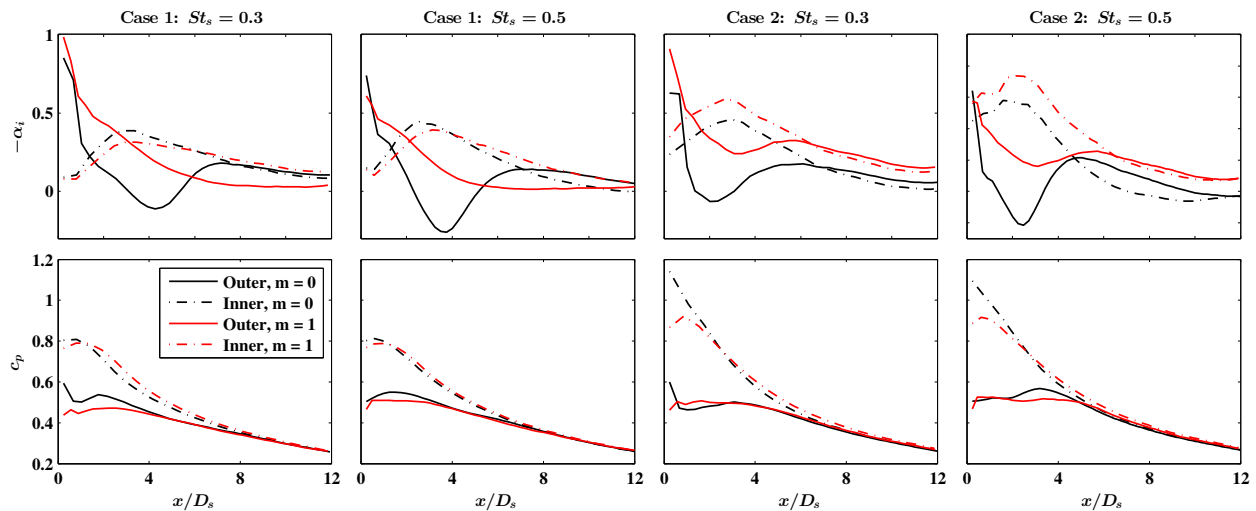


Figure 5. Growth rate and phase speed of outer and inner PSE solutions for representative  $St_s - m$  pairs in both cases 1 and 2.

two azimuthal modes, and it is also known to be less important for sound radiation in single-stream jets.<sup>7</sup> Hence, PSE results are only presented for  $m = 0$  and  $m = 1$ .

## B. PSE results

We initiate separate PSE calculations from the inner and outer unstable LST eigensolutions at  $x = 0.25D_s$  described in § A for various pairs of frequencies and azimuthal modes. The PSE method tracks the instability as it marches downstream. Whereas the outcome is unambiguous when a single unstable mode is present, the result is confused if the base flow supports multiple instabilities (as is the case here). Note that the primary and secondary shear layers merge some distance downstream of the nozzle exit, and thus cannot support multiple unstable Kelvin-Helmholtz modes thereat (in the sense of parallel-flow LST).

To elucidate this point, fig. 5 shows the growth rate and phase speed of the outer and inner PSE solutions for two representative frequencies and the two lowest azimuthal modes in both cases 1 and 2. We notice that the  $m = 0$  outer mode solution decays quickly but becomes slightly unstable again further downstream before tracking the decay of the corresponding inner mode. The phase speeds of the two modes also collapse downstream on one curve. This clearly demonstrates the coalescence of the outer and inner modes. That is, although they start out as distinct instabilities near the nozzle, PSE cannot track them separately after the outer mode stabilizes. The coalescence occurs around  $x = 8D_s$  for Case 1 and  $x = 6D_s$  for Case 2. The same behaviour is also exhibited by the  $m = 1$  solution, but more prominently in Case 2. In Case 1, the  $m = 1$  outer and inner modes remain distinct almost till the end of the domain. These observations are representative of the range of frequencies studied ( $0.05 \leq St_s \leq 1.0$ ).

To explain the above differences, we recall that  $m = 1$  mode remains unstable whereas  $m = 0$  mode stabilizes in the more gradual shear profiles encountered at downstream sections of round jets.<sup>26</sup> In fact, we observe this again in the present results in the lack of stabilization of the  $m = 1$  modes (both outer and inner) even by the end of the calculation domain; the  $m = 0$  outer mode stabilizes much earlier. Moreover, the merger of the outer and inner modes of  $m = 0$  is also delayed in Case 1 compared to Case 2. Combining these two observations, we can explain the much delayed merger of the outer and inner modes of  $m = 1$  in Case 1.

To summarize, the merger of the outer and inner solutions reflects a confluence of two factors: (1) the merger of the outer and inner shear layers whereby the base flow supports only a single unstable K-H mode (in the sense of parallel-flow LST), and (2) the stabilization of the outer mode whence this PSE solution falls into the basin of attraction of the unstable inner mode. Based on the foregoing discussion, we will limit the outer mode calculations to  $x = 8D_s$  for Case 1 and  $x = 6D_s$  for Case 2. The inner modes will be calculated till  $x = 12D_s$ . Ideally, the outer mode calculations should be terminated at different axial stations for different  $St_s - m$  pairs (lower frequency modes stabilize further downstream); however, we make

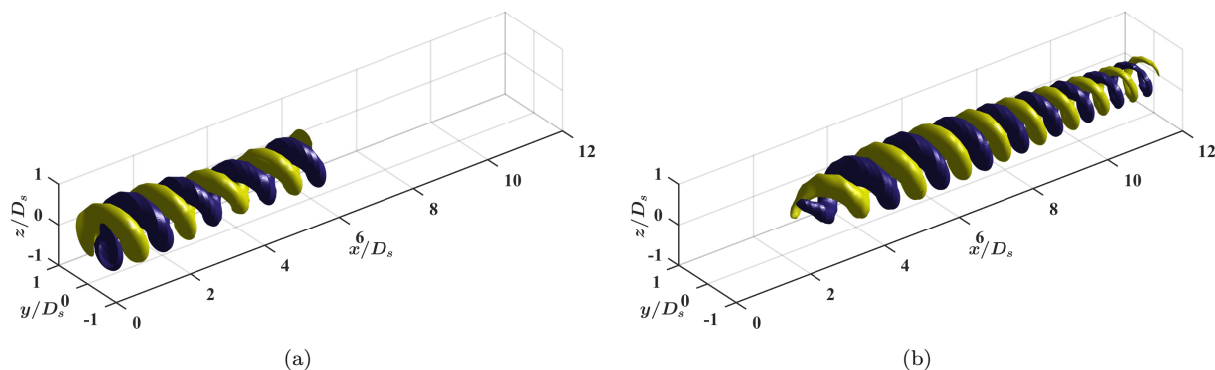


**Figure 6.** Representative positive and negative isosurfaces of the real part of pressure in the (a) outer, and (b) inner mode PSE solutions for  $St_s = 0.5$ ,  $m = 1$ . The outer mode calculations are terminated at  $x = 6D_s$ .

the above uniform choice for ease of the discussion.

Figure 6 presents a visualization of the outer and inner mode PSE solutions for  $St_s = 0.5$ ,  $m = 1$  through representative isosurfaces of the pressure component. Pressure, being a global variable, evinces the coherent wavepacket structure most clearly.<sup>3</sup> We observe the wavepacket nature here too – the overall amplitude increases to saturation and then decays, whereas the wavelength is approximately uniform throughout. We also note that the outer mode peaks earlier compared to the inner mode (at  $\sim 1.5D_s$  as opposed to  $\sim 4.5D_s$ ) and has a longer wavelength ( $\sim 1.4D_s$  vs.  $\sim 1.1D_s$ ).

The linear PSE solution represents a coherent fluctuation over the entire domain. However, the actual turbulence is nowhere nearly as coherent. To have a meaningful comparison between our theory and the LES data, we must therefore extract the coherent part of the turbulent fluctuations. We do this using proper orthogonal decomposition (POD), originally introduced to the fluid dynamics community in Ref. 27. POD has been used successfully to extract coherent wavepackets from turbulence to validate stability results for round subsonic<sup>8,2</sup> and supersonic jets,<sup>10</sup> as well as for subsonic jets issuing from nozzles with chevrons.<sup>22</sup>

We now provide a brief review of POD as applied to the LES data. The LES time-series over the entire spatial domain is divided into segments of duration  $20D_s/U_s$  with 75% overlap. The pressure data in each segment is Fourier transformed in time and azimuth. The subsequent steps follow the snapshot POD method,<sup>28</sup> with the frequency-and-azimuthal Fourier domain data obtained above treated as independent snapshots of the turbulent fluctuations. In particular, we define the inner product such that the induced norm is the pressure fluctuation energy (for each  $St_s - m$  pair) over the chosen cylindrical domain. Once the spatial domain is discretized, the POD problem reduces to a positive semi-definite symmetric matrix eigenvalue problem. The  $n$ th largest (real) eigenvalue (denoted  $\lambda_{\omega,m}^n$ ) is associated with the POD eigenfunction (denoted  $\Phi_{\omega,m}^n(x,r)$ ) that is  $n$ th in descending order of prevalence in the turbulence.

Some representative outer and inner mode PSE results (the real parts of their pressure component) are shown in fig. 7 for a few  $St_s - m$  mode pairs for both Cases 1 and 2. In the linear PSE calculations, the overall amplitude of the wavepackets is indeterminate; hence we only make note of the shape of the contours and their relative levels.

We observe that, with increasing Strouhal number, the wavelength reduces and the wavepackets become more compact both axially and radially. The first behavior reflects the approximately similar phase speeds within the same instability family, and is extensively reported in the literature of round jets. It is also noted that, the axisymmetric modes saturate and decay earlier compared to the first helical modes, as has also been reported earlier. Moreover, the outer modes display broader radial coherence than the inner modes (as they do in the LST eigensolutions at the initial station). Furthermore, the inner mode peaks significantly later compared to the outer mode, as noted in fig. 6. It appears to be strong over a longer axial domain of the jet. Finally, we find that the wavelengths of the inner and outer modes are substantially similar (the difference noted in fig. 6 is subtle).

The main purpose of fig. 7 is to compare qualitatively the PSE solutions with the nearest low-order coherent POD mode of the LES data. For this comparison, the overall amplitudes (which are indeterminate anyway) are set as follows. First, the POD modes are individually normalized so that they take values from  $-1$  to  $+1$ . Then, the PSE solutions' overall amplitudes are determined to minimize the difference (in

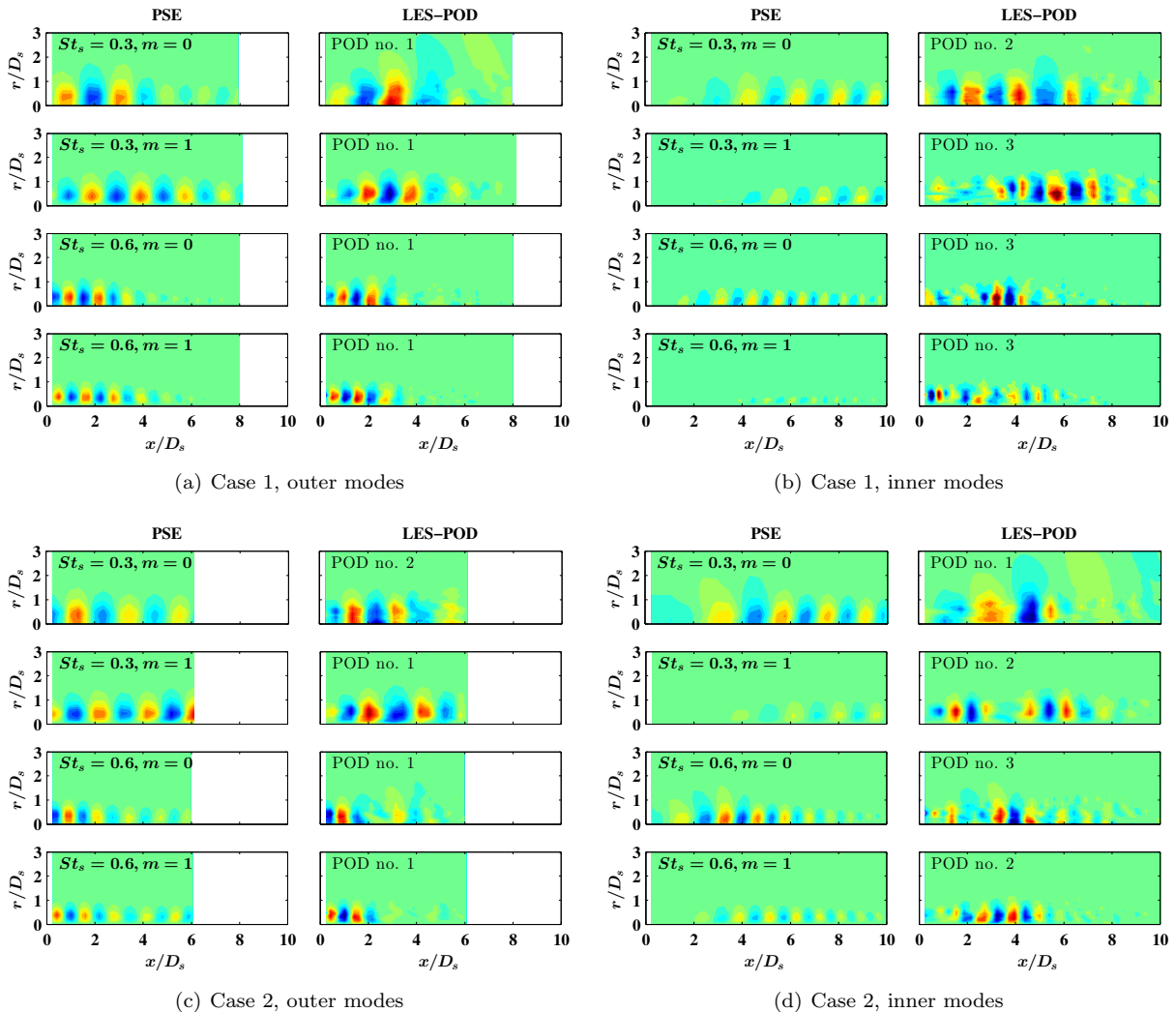


**Figure 7.** Real parts of pressure PSE solutions (left columns) and POD modes of LES data (right columns) for some  $St_s - m$  mode pairs (see titles in left column figures) for outer and inner modes in Cases 1 and 2. All fields are normalized to the same range, so that they take values from  $-1$  to  $+1$ . Different POD mode numbers of the data that are closest to the solution are presented, as indicated in the right column figures.

the least-squares sense) of their pressure fields from the corresponding POD modes (see Ref. 10, 22 for the details of this procedure). The comparison is made with the low-order (most prevalent) POD mode that most resembles the PSE solution (the determination of this ‘resemblance’ is described below in the quantitative analysis).

We observe that the outer modes from the PSE calculations display reasonable similarity with the coherent part of the data, for both Cases 1 and 2. The inner modes predicted by the model, especially in Case 1 and more so for  $m = 1$ , cannot be reliably detected in the data.

Before pursuing a quantitative validation of the PSE solutions, we first establish the significance of the POD modes of the data. To this end, fig. 8(a) presents the coherence of the LES data, as measured by the fraction of ‘energy’ in the three lowest pressure POD modes ( $\lambda^n / \sum_i \lambda^i$ ). We display results for both Cases 1 and 2, and for the relevant choices of the axial domain extent (‘Outer’ refers to the domain ending at  $x = 8D_s$  and  $6D_s$  for the respective cases, and ‘Inner’ refers to the domain ending at  $12D_s$  in both cases).

We observe that across the range of Strouhal numbers  $St_s$  and the two azimuthal modes, Case 1 is more coherent (POD mode 1 represents a larger fraction) compared to Case 2. Also, the decay of coherence with increasing  $St_s$  is steeper in Case 2. In fact, in Case 2, the first two POD modes have similar coherence for  $St_s \gtrsim 0.6$ . The different axial domains considered do not make a significant impact on the coherence of

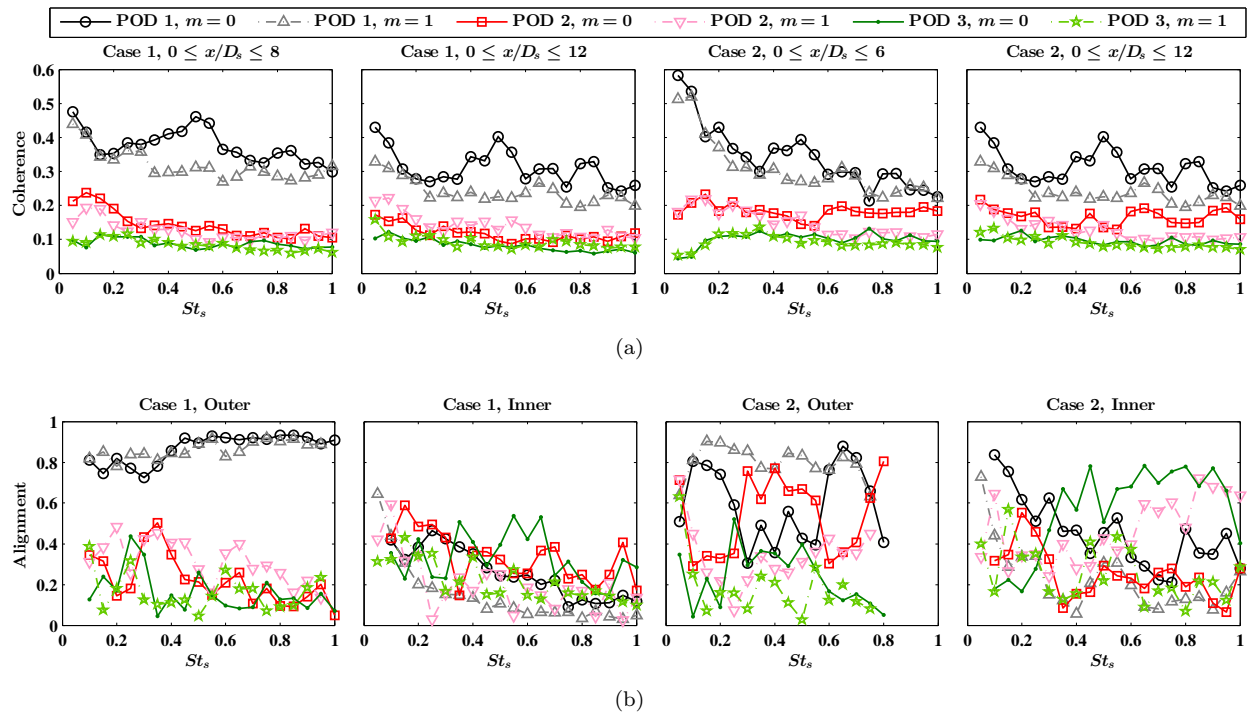


Figure 8. (a) Coherence of first three pressure POD modes in cases 1 & 2 over a range of frequencies for  $m = 0$  and 1. Two axial domain extents are used for the POD calculations in both cases, as these are respectively relevant for comparison with outer and inner PSE solutions. (b) Alignment of the pressure component of the PSE solutions with the POD modes presented in (a).

depicted POD modes. Overall, we conclude that the least-order POD modes represent a significant coherent portion of the turbulent fluctuations, so that validation of the PSE solutions against them assures of a useful model.

Since the overall amplitude of the wavepackets cannot be determined by *linear* PSE, a suitable metric for comparison is the ‘alignment’<sup>10</sup> of the PSE solution with the  $n$ th POD mode for an  $St_s - m$  pair:

$$\mathcal{A}_{m,\omega}^n := \frac{\left| \left\langle \hat{q}_{\omega,m}, \hat{\Phi}_{m,\omega}^n \right\rangle \right|}{\left\| \hat{q}_{\omega,m} \right\| \left\| \hat{\Phi}_{m,\omega}^n \right\|}. \quad (2)$$

Since the POD modes form an orthogonal basis, the above definition implies that  $0 \leq \mathcal{A}^n \leq 1$ . A value close to unity for the first POD mode indicates that the PSE solution is structurally similar to the most prevalent coherent wavepacket found in the flow, and so on.

The alignment metric is evaluated for the first three POD modes and the results are presented in fig. 8(b). The clearest alignment is observed in Case 1 for the outer mode (with the first POD mode) for both  $m = 0$  and 1. Correspondingly, the worst alignment is noted for the inner modes in the same case. We conjecture that this is related to the lack of velocity shear in the inner shear layer in this case (there is only a temperature shear), which makes the inner mode unimportant to the turbulent dynamics of this jet. However, the outer mode can be detected clearly in the turbulence, attesting to its relevance.

In Case 2, we notice that the  $m = 0$  outer mode is aligned to the *second* POD mode over an intermediate range of frequencies, and to the first POD mode over the remaining range. To study this case in detail, we show the first three POD modes for  $m = 0$  in Case 2 over this range of frequencies in fig. 9. The POD mode 1 for  $St_s = 0.3, 0.4$  and  $0.5$  and the POD mode 2 for  $St_s = 0.6$  (those POD modes that do *not* agree with the outer mode PSE solution) display significant acoustic radiation that is coherent with the hydrodynamic wavepacket. This character was missing from Case 1 results – the salient difference between the two cases is of course the faster inner stream in Case 2. This causes more efficient transfer of turbulent energy to acoustics in Case 2.<sup>3</sup> However, the jet is still convectively subsonic (see, for example, the phase speed evolution in

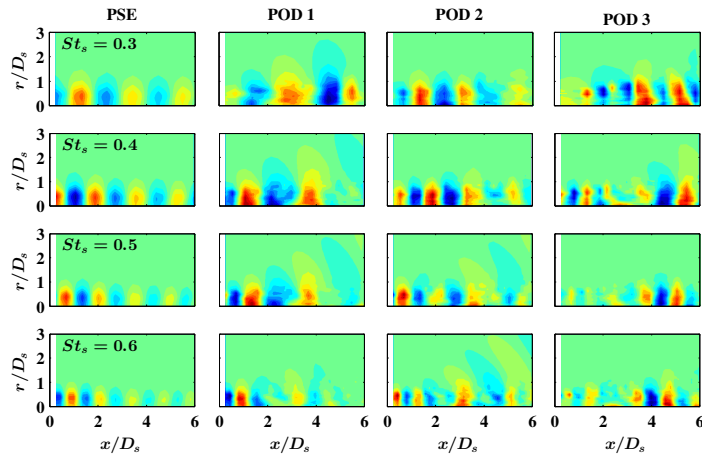


**Figure 9.** Comparison of the outer mode PSE pressure solution with the first three pressure POD modes of four frequencies in  $m = 0$  of Case 2. The POD calculations are limited to the axial domain up to  $x = 6D_s$ .

fig. 5), and PSE cannot retrieve the acoustic solution thereof. In case of convectively supersonic round jets (as studied in Ref. 10), PSE can correctly capture the acoustic radiation from the wavepackets.

Returning to the remaining Case 2 solutions in fig. 8, the  $m = 1$  outer mode PSE solution is well aligned with the corresponding first POD mode. The  $m = 0$  inner mode solutions are aligned with the third POD mode for  $St_s \gtrsim 0.35$  (recall that the corresponding outer modes are aligned with the second POD modes, and that the first POD mode has significant acoustic character). The  $m = 1$  inner mode PSE solutions demonstrate mild alignment with the corresponding second POD modes for  $St_s \gtrsim 0.6$ . The agreement of the inner mode PSE solutions with the data is much better in Case 2 compared to Case 1. This reflects again the greater velocity gradients in the inner shear layer of the former, such that the inner mode has greater energy (prevalence) in the turbulent flow field.

## V. Conclusions

In this paper, we pursue the modeling of coherent wavepackets in dual-stream axisymmetric high-speed high-Reynolds number jets of realistic geometry. Such wavepackets have been conclusively found in round jets and even in jets issuing from serrated nozzles, and have been linked to the dominant mixing noise radiation thereof. The wavepackets are modeled as linear instabilities of the turbulent mean flow using parabolized stability equations (PSE). The overall motivation is to arrive at a reduced-order model for rapidly predicting the approximate acoustic field of dual-stream jets.

The base flow for the stability analysis is taken from a new LES database of the dual-stream jet. Two operating conditions (referred to as Cases 1 and 2) are simulated – both have a hot inner core stream and both have subsonic local Mach number. However, the inner stream in Case 2 has supersonic acoustic Mach number.

In the sense of locally-parallel linear stability theory, the base flow near the nozzle exit supports two unstable modes corresponding to the two inflection points – these are called inner and outer modes following Ref. 15. It is well known that PSE cannot distinguish between two unstable modes if their complex wavenumbers are too similar, or if one stabilizes during the downstream march whereas the other remains unstable. This is precisely the challenge in the present work – to analyze the PSE results initiated from the inner and outer mode instabilities at a near-nozzle station, and to validate the results with the LES data.

Under the two operating conditions considered, the outer PSE solution can be distinctly observed in the LES data once the latter is filtered for the coherent part using proper orthogonal decomposition (POD). The inner mode PSE solution in Case 2 (with steeper gradient in the inner shear layer) is also discernible to an extent in the LES data, but not so for Case 1. This is linked to the lower energy (prevalence) of the inner mode in Case 1, owing to the milder gradient in the inner shear layer thereof.

**Acknowledgements:** The authors thank Kristjan Gudmundsson, Arnab Samanta, Daniel Rodríguez and Tim Colonius for contributing to the development of the PSE code for the round jet. AS acknowledges support from Industrial Research and Consultancy Center of Indian Institute of Technology Bombay, via the seed grant program.

## References

- <sup>1</sup>Papamoschou, D. and Debiasi, M., “Directional suppression of noise from a high-speed jet,” *AIAA Journal*, Vol. 39, No. 3, 2001, pp. 380–387.
- <sup>2</sup>Cavalieri, A. V. G., Jordan, P., Colonius, T., and Gervais, Y., “Axisymmetric superdirectivity in subsonic jets,” *Journal of Fluid Mechanics*, Vol. 704, 2012, pp. 388–420.
- <sup>3</sup>Jordan, P. and Colonius, T., “Wave packets and turbulent jet noise,” *Annu. Rev. Fluid Mech.*, Vol. 45, 2013, pp. 173–195.
- <sup>4</sup>Crighton, D. G. and Gaster, M., “Stability of slowly diverging jet flow,” *Journal of Fluid Mechanics*, Vol. 77, No. 2, 1976, pp. 397–413.
- <sup>5</sup>Mankbadi, R. and Liu, J. T. C., “Sound generated aerodynamically revisited: large-scale structures in a turbulent jet as a source of sound,” *Proc. R. Soc. Lond. A*, Vol. 311, No. 1516, 1984, pp. 183–217.
- <sup>6</sup>Tam, C. K. W. and Burton, D. E., “Sound generated by instability waves of supersonic flows. Part 1. Two-dimensional mixing layers,” *Journal of Fluid Mechanics*, Vol. 138, 1984, pp. 249–271.
- <sup>7</sup>Suzuki, T. and Colonius, T., “Instability waves in a subsonic round jet detected using a near-field phased microphone array,” *Journal of Fluid Mechanics*, Vol. 565, 2006, pp. 197–226.
- <sup>8</sup>Gudmundsson, K. and Colonius, T., “Instability wave models for the near-field fluctuations of turbulent jets,” *Journal of Fluid Mechanics*, Vol. 689, 2011, pp. 97–128.
- <sup>9</sup>Cavalieri, A. V. G., Rodríguez, D., Jordan, P., Colonius, T., and Gervais, Y., “Wavepackets in the velocity field of turbulent jets,” *Journal of Fluid Mechanics*, Vol. 730, 2013, pp. 559–592.
- <sup>10</sup>Sinha, A., Rodríguez, D., Brès, G., and Colonius, T., “Wavepacket models for supersonic jet noise,” *Journal of Fluid Mechanics*, Vol. 742, 2014, pp. 71–95.
- <sup>11</sup>Dahl, M. D. and Morris, P. J., “Noise from supersonic coaxial jets. Part 2: Normal velocity profile,” *Journal of Sound and Vibration*, Vol. 200, No. 5, 1997, pp. 665–699.
- <sup>12</sup>Saric, W. S. and Nayfeh, A. H., “Nonparallel stability of boundary-layer flows,” *Physics of Fluids*, Vol. 18, No. 8, 1975, pp. 945–950.
- <sup>13</sup>Dahl, M. D. and Papamoschou, D., “Analytical predictions and measurements of the noise radiated from supersonic coaxial jets,” *AIAA journal*, Vol. 38, No. 4, 2000, pp. 584–591.
- <sup>14</sup>Perrault-Joncas, D. and Maslowe, S. A., “Linear stability of a compressible coaxial jet with continuous velocity and temperature profiles,” *Physics of Fluids*, Vol. 20, 2008, pp. 074102.
- <sup>15</sup>Gloor, M., Obrist, D., and Kleiser, L., “Linear stability and acoustic characteristics of compressible, viscous, subsonic coaxial jet flow,” *Physics of Fluids*, Vol. 25, 2013, pp. 084102.
- <sup>16</sup>Léon, O. and Brazier, J.-P., “Investigation of the near and far pressure fields of dual-stream jets using an Euler-based PSE model,” *19th AIAA/CEAS Aeroacoustics Conference, AIAA Paper 2839*, 2013.
- <sup>17</sup>Tinney, C. E. and Jordan, P., “The near pressure field of co-axial subsonic jets,” *Journal of Fluid Mechanics*, Vol. 611, 2008, pp. 175–204.
- <sup>18</sup>Vuillot, F., Lupoglazoff, N., and Rahier, G., “Double-stream nozzles flow and noise computations and comparisons to experiments,” *46th AIAA Aerospace Sciences Meeting and Exhibit, AIAA Paper 9*, 2008.
- <sup>19</sup>Bogey, C., Barré, S., Juvé, D., and Bailly, C., “Simulation of a hot coaxial jet: Direct noise prediction and flow-acoustics correlations,” *Physics of Fluids*, Vol. 21, No. 3, 2009, pp. 035105.
- <sup>20</sup>Eastwood, S. J. and Tucker, P. G., “Hybrid LES – RANS of complex geometry jets,” *International Journal of Aeroacoustics*, Vol. 10, 2011, pp. 659–684.
- <sup>21</sup>Bertolotti, F. P. and Herbert, T., “Analysis of the linear stability of compressible boundary layers using the PSE,” *Theoretical and Computational Fluid Dynamics*, Vol. 3, No. 2, 1991, pp. 117–124.
- <sup>22</sup>Sinha, A., Gudmundsson, K., Xia, H., and Colonius, T., “Parabolized stability analysis of jets from serrated nozzles,” *Journal of Fluid Mechanics*, Vol. 789, 2016, pp. 36–63.
- <sup>23</sup>Li, F. and Malik, M. R., “Spectral analysis of parabolized stability equations,” *Computers & Fluids*, Vol. 26, No. 3, 1997, pp. 279–297.
- <sup>24</sup>Gaitonde, D. V. and Samimy, M., “Coherent structures in plasma-actuator controlled supersonic jets: axisymmetric and mixed azimuthal modes,” *Physics of Fluids*, Vol. 23, 2011, pp. 095104.
- <sup>25</sup>Gaitonde, D. V. and Visbal, M. R., “Padé-type higher-order boundary filters for the Navier-Stokes equations,” *AIAA Journal*, Vol. 38, No. 11, 2000, pp. 2103–2112.
- <sup>26</sup>Batchelor, G. K. and Gill, A. E., “Analysis of the stability of axisymmetric jets,” *Journal of Fluid Mechanics*, Vol. 14, No. 4, 1962, pp. 529–551.
- <sup>27</sup>Lumley, J. L., “The structure of inhomogeneous turbulent flows,” *Atm. Turb. and Radio Wave Prop.*, edited by A. M. Yaglom and V. I. Tatarsky, Nauka, Moscow, 1967, pp. 166–178.
- <sup>28</sup>Sirovich, L., “Turbulence and the dynamics of coherent structures, Parts I-III,” *Quarterly of Applied Mathematics*, Vol. XLV, No. 3, 1987, pp. 561–590.